2013 IEEE International Conference on Control Applications (CCA)
Part of 2013 IEEE Multi-Conference on Systems and Control
Hyderabad, India, August 28-30, 2013

Path Generation and Integrated Guidance and Control of a Micro Air Vehicle

K. Harikumar[1] and M.Seetharama Bhat[2]

Abstract— **In this paper, we consider the problem of generating a feasible path connecting two waypoints in a three dimensional space with specified heading and flight path angles for a fixed wing micro air vehicle (MAV). The algorithm is based on simple geometric construction and can be used for generating paths for in flight waypoints. The guidance law used here is a modified version of the PN guidance law. Due to the strong coupling between the lateral and longitudinal dynamics and low actuator bandwidth, an integrated framework for guidance and control is also developed.**

I. INTRODUCTION

Micro air vehicles (MAV) have typical take off weight less than 200g and wing span less than 300mm. Navigation and control of such vehicles are difficult due to their small size, and large disturbances as compared to their inertial and control forces. In any of the MAV applications, it has to reach set of waypoints, specified by the end user. The orientation of the vehicle at each waypoint may be specified depending on the mission requirements. The guidance law generates the guidance commands to follow the path connecting the waypoints. These guidance commands are the set points for the inner loop control system. Alternatively, the guidance and control can be combined to form a single integrated guidance and control logic.

The problem of path planning consists of generating a feasible path between the waypoints, that can be followed by the vehicle without violating its climb rate and acceleration limits. Many path planning algorithms are available in the literature. Computational complexity and optimality are the key issues based on which different algorithms can be evaluated. Such an algorithm should be able to generate a solution in real time with limited onboard computational resources. Optimal algorithm chooses the best solution from the available solutions based on a specified performance criterion. For example, minimum path length or minimum time taken to travel are the popular performance measures.

An algorithm for trajectory planning for UAV between the given waypoints in three dimensional space has been explained in [1]. It uses the kinematic model of the vehicle to generate trajectories through mid course waypoints. The algorithm requires numerical solution of six coupled non linear differential equations. In [2], waypoint navigation is achieved through a fusion of pursuit guidance law and the idea of virtual target. The pursuit guidance generates very high acceleration commands when the UAV is near the target and that might not be achievable for MAVs. In [3], a trajectory optimization problem is solved using pseudospectral method for waypoint navigation. The algorithms in [1] and [3] are computationally expensive for real time implementation in a small on board computer in MAVs. In [4], the 3D path generation problem is broken into 3 subpaths each in a 2D plane. It generates a feasible path, but the splitting into 3 subpaths makes the total path length longer . In [5], an optimal path is generated between two waypoints using a simple geometric construction but that does not guarantee a flyable path for the MAV. In all the above methods, the heading and flight path angles generated are given to the lateral and longitudinal autopilot respectively as a reference command to track. They assume that the kinematics and dynamics are decoupled and the control system has very large band width enabling it to track the guidance commands. But in the case of MAVs, time scale separation between the kinematics and dynamics are small and there is a strong coupling between the longitudinal and lateral dynamics. Moreover, the actuators are of low bandwidth making the overall system bandwidth comparable to the outer loop. This problem can be handled by integrating the guidance and control function into a single loop design. In [6], an integrated guidance and control framework is used for tracking trim trajectories. But the algorithm can track only helical paths and has a singularity when following straight line paths. In this paper, a new method is proposed for obtaining a feasible path between the MAV current position to a desired waypoint in a three dimensional space with specified final heading and flight path angles. The derived path lies in two tilted planes in a 3D space. A guidance logic, which is a modified version of PN guidance law is embedded as a part of control logic for tracking the path. The kinematics and dynamics are combined to form a single twelve degree of freedom model, thus integrating the guidance and control design. The paper is organized as follows. § II deals with the generation of a feasible path connecting the current MAV location to the desired waypoint position in 3D space and the guidance logic. In § III, the integrated guidance and control frame work is derived. Simulation results are presented in § IV.

II. Path generation algorithm

Here the MAV is assumed to be flying at a constant speed. In the figure 1, (X_I, Y_I, Z_I) is the inertial frame. The input to the algorithm are the current position (x_0, y_0, z_0), initial

[1] K.Harikumar is a research scholar in Department of Aerospace Engineering, Indian Institute of Science, Bangalore 560012, India. harikumar@aero.iisc.ernet.in

[2] M.Seetharama Bhat is a Professor in Department of Aerospace Engineering, Indian Institute of Science, Bangalore 560012, India. msbdcl@aero.iisc.ernet.in

978-1-4799-1559-0/13/$31.00 ©2013 IEEE

velocity vector (V_1), heading ψ_0 and flight path angle γ_0 of the MAV and the next waypoint position (x_f, y_f, z_f), the final velocity vector (V_2), the required heading ψ_f and flight path angle γ_f upon reaching the waypoint. The entire path to be followed by the MAV is projected on to the two planes. The MAV will be initially flying in the first plane defined by the initial velocity vector and the vector joining the initial position and the final position as in figure 1. The second portion of the flying path will be in another plane defined by final desired velocity vector and the vector joining the initial position and the final position as in figure 1. $X_{p1}Y_{p1}Z_{p1}$ and $X_{p2}Y_{p2}Z_{p2}$ are the frames attached to the first plane and the second plane respectively and are defined below. The transition from the first plane to the second plane happens when the velocity vector of the MAV gets aligned to the line joining the initial MAV position and the next waypoint. Let P_{01} be the point of switching from first plane to the second plane and V_{01} be the velocity vector at the instant of switching. The algorithm for generation of the path is explained below. Let the origin of the inertial frame be shifted to (x_0, y_0, z_0). Then the next waypoint position becomes $x_2 = (x_f - x_0), y_2 = (y_f - y_0), z_2 = (z_f - z_0)$. The first plane called PL_1 is drawn in figure 2. Here $(0,0,0)$ is the origin of the PL_1 plane, $X_{p1}Y_{p1}Z_{p1}$ is a frame attached to the plane, dotted line represents a typical path generated as per the guidance logic explained below, $(x_{f1}, y_{f1}, 0)$ and $(x_{01}, y_{01}, 0)$ are two points in the line AB where the path intersects, ζ is the angle which the line AB makes with V_1 and $(x'_2, y'_2, 0)$ is the next waypoint position expressed in the frame $X_{p1}Y_{p1}Z_{p1}$. Let (x,y,z) be any point in the PL_1 plane. The equation of the PL_1 plane is given by

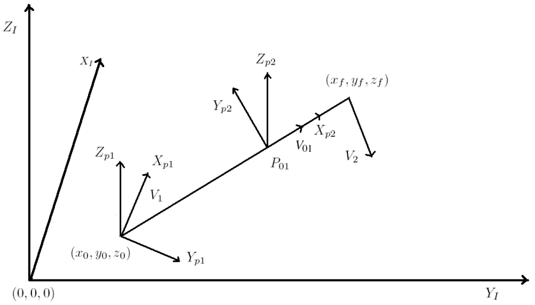

Fig. 1. 3D geometry for two waypoints

$$A_1x + B_1y + C_1z = 0 \tag{1}$$

where

$$A_1 = y_2\,sin\gamma_0 - z_2\,sin\psi_0\,cos\gamma_0 \tag{2}$$

$$B_1 = z_2\,cos\psi_0\,cos\gamma_0 - x_2\,sin\gamma_0 \tag{3}$$

$$C_1 = x_2\,sin\psi_0\,cos\gamma_0 - y_2\,cos\psi_0\,cos\gamma_0 \tag{4}$$

Let a new frame $X_{p1}Y_{p1}Z_{p1}$ be defined with X_{p1} axis along the current velocity vector $(cos\psi_0\,cos\gamma_0, sin\psi_0\,cos\gamma_0, sin\gamma_0)$ of the MAV, Y_{p1} axis orthogonal to X_{p1} axis on the PL_1 plane and Z_{p1} axis given by $X_{p1} \times Y_{p1}$. Let the unit vector along Y_{p1} axis be (a,b,c). Since (a,b,c) is orthogonal to $(cos\psi_0 cos\gamma_0, sin\psi_0 cos\gamma_0, sin\gamma_0)$ and lies in the PL_1 plane,

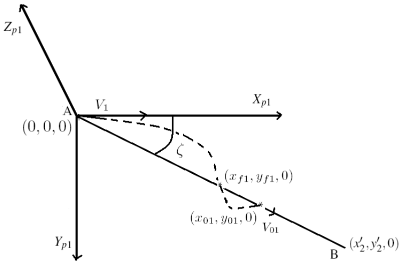

Fig. 2. Diagram explaining path generation in the PL_1 plane

$$a\,cos\psi_0\,cos\gamma_0 + b\,sin\psi_0\,cos\gamma_0 + c\,sin\gamma_0 = 0 \tag{5}$$

$$aA_1 + bB_1 + cC_1 = 0 \tag{6}$$

$$tan\zeta = \frac{ax_2 + by_2 + cz_2}{x_2\,cos\psi_0\,cos\gamma_0 + y_2\,sin\psi_0\,cos\gamma_0 + z_2\,sin\gamma_0} \tag{7}$$

Solve the linear equations 5,6 and 7 to obtain (a,b,c). Let the unit vector along Z_{p1} axis be (a_1, b_1, c_1) and is given by $X_{p1} \times Y_{p1}$. The rotation matrix ${}^{I}R_{P_1}$ from the $X_{p1}Y_{p1}Z_{p1}$ frame to the inertial frame is given by,

$${}^{I}R_{P_1} = \begin{pmatrix} cos\psi_0\,cos\gamma_0 & a & a_1 \\ sin\psi_0\,cos\gamma_0 & b & b_1 \\ sin\gamma_0 & c & c_1 \end{pmatrix} \tag{8}$$

Let the airspeed be V_a. Since the MAV flies at a constant speed, $\mid V_1 \mid = \mid V_{01} \mid = \mid V_2 \mid = V_a$. It is possible to maintain near or constant airspeed using engine throttle. The kinematics of the MAV with respect to $X_{p1}Y_{p1}Z_{p1}$ frame is

$$\dot{x_{p1}} = V_a sin(\psi_1);\ \dot{y_{p1}} = V_a cos(\psi_1);\ z_{p1} = 0;\ \dot{\psi_1} = \frac{a_c}{V_a} \tag{9}$$

Here a_c is the acceleration command and is obtained from the guidance law as explained below. In figure 3, $X'Y'$ is parallel to $X_{p1}Y_{p1}$, $(x_{p1}, y_{p1}, 0)$ is the MAV current position in the PL_1 plane, $(x_{fa}, y_{fa}, 0)$ is a point in the PL_1 plane, r_a is the range, σ is the angle between the line AB and X' axis, ψ_1 is the angle made by the velocity vector with the Y' axis and d is the perpendicular distance between the velocity vector and $(x_{fa}, y_{fa}, 0)$. The acceleration applied is perpendicular to the velocity vector and lies in the PL_1 plane.

$$\sigma = tan^{-1}\left(\frac{y_{fa} - y}{x_{fa} - x}\right); \quad \rho = \frac{\pi}{2} - (\psi_1 + \sigma) \tag{10}$$

$$r_a = \sqrt{(x - x_{fa})^2 + (y - y_{fa})^2};\ d = r_a sin\rho \tag{11}$$

$$a_c = k_1 d + k_2 \dot{d} \tag{12}$$

Here k_1 and k_2 are navigational constants of an equivalent zero effort miss (ZEM) guidance logic. The MAV will take a turning trajectory to reach the line AB. Let the minimum

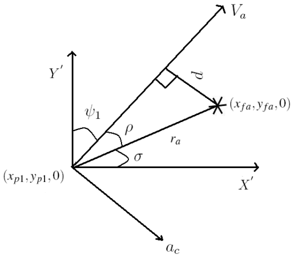

Fig. 3. Diagram explaining the guidance logic

turn radius of the vehicle be R_{min}. The value of R_{min} in pitch plane and yaw plane depends upon longitudinal and lateral acceleration capabilities of MAV, which will have impact on stall angle of attack and side slip angle as well as limits on elevator and rudder deflections. Now the MAV has to turn in a tilted plane with respect to the inertial frame. So choose a turn radius $R > R_{min}$ and the maximum acceleration becomes $a_{cmax} = \frac{V_a{}^2}{R}$. Let a point $(x_{f1}, y_{f1}, 0)$ lying on the line AB (ref figure 2), which is at a distance 2R from the origin of the PL_1 plane be the point at which the MAV has to reach first.

$$m = tan\zeta; \;\; x_{f1} = \frac{2R}{\sqrt{1+m^2}}; \;\; y_{f1} = mx_{f1} \tag{13}$$

The path followed by the MAV is not unique and depends upon the parameters k_1 and k_2 used in the acceleration command. To get the MAV velocity vector aligned to the line AB, a second point in the line AB is commanded. A typical path followed by the MAV in the PL_1 plane is shown as dotted lines in the figure 2. Let the coordinate where the velocity vector gets aligned to the line AB be $(x_{01}, y_{01}, 0)$, the corresponding coordinate in the inertial frame is given by $P_{01} = {}^{I}R_{P_1}(x_{01}, y_{01}, 0)^T$. Then $(x_2', y_2', 0)^T = ({}^{I}R_{P_1})^{-1}(x_2, y_2, z_2)^T$. A second plane called PL_2 (ref figure 4), is defined by the final desired velocity vector $(cos\psi_f\, cos\gamma_f,\, sin\psi_f\, cos\gamma_f,\, sin\gamma_f)$ and the vector joining the initial position $(0,0,0)$ and the final MAV position (x_2, y_2, z_2). Here $X_{p2}Y_{p2}Z_{p2}$ is a new frame attached to the PL_2 plane and $(x_2'', y_2'', 0)$ is the next waypoint position expressed in this frame. The dotted lines represents a typical path generated in the PL_2 plane consisting of a curve, straight line and a circle up to the points $1'$, $(m_0, n_0, 0)$ and $(x_2'', y_2'', 0)$ respectively and are obtained as explained below. Let (x, y, z) be any point in the PL_2 plane. The equation of the PL_2 plane is given by

$$A_2 x + B_2 y + C_2 z = 0 \tag{14}$$

where

$$A_2 = y_2\, sin\gamma_f - z_2\, sin\psi_f\, cos\gamma_f \tag{15}$$

$$B_2 = z_2\, cos\psi_f\, cos\gamma_f - x_2\, sin\gamma_f \tag{16}$$

$$C_2 = x_2\, sin\psi_f\, cos\gamma_f - y_2\, cos\psi_f\, cos\gamma_f \tag{17}$$

Let the velocity vector at the point P_{01} be given by $V_{01} = (V_a cos\psi_{01} cos\gamma_{01}, V_a sin\psi_{01} cos\gamma_{01}, V_a sin\gamma_{01})$, where

$$\gamma_{01} = tan^{-1}\Big(\frac{z_2}{\sqrt{(x_2)^2 + (y_2)^2}}\Big); \;\; \psi_{01} = tan^{-1}\Big(\frac{y_2}{x_2}\Big) \tag{18}$$

Now define a new frame $X_{p2}Y_{p2}Z_{p2}$ on the PL_2 plane (ref. figure 4) with X_{p2} axis along the current velocity vector of the MAV, Y_{p2} axis, orthogonal to X_{p2} axis on the PL_2 plane and Z_{p2} axis given by $X_{p2} \times Y_{p2}$. The Y_{p2} and Z_{p2} axis can be obtained as follows. Let a plane perpendicular to current velocity vector be PL_3 and is given by,

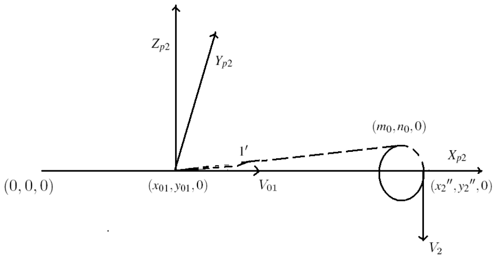

Fig. 4. Diagram explaining path generation in the PL_2 plane

$$A_3 x + B_3 y + C_3 z + D_3 = 0 \tag{19}$$

where

$$A_3 = cos\psi_{01}\, cos\gamma_{01}; \;\; B_3 = sin\psi_{01}\, cos\gamma_{01} \tag{20}$$

$$C_3 = sin\gamma_{01}; \;\; D_3 = -P_{01}[A_3, B_3, C_3]^T \tag{21}$$

The intersecting line between the planes PL_2 and PL_3 gives the Y_{p2} axis and is given by cross product of (A_2, B_2, C_2) and (A_3, B_3, C_3).

$$A_4 = B_2C_3 - C_2B_3; B_4 = C_2A_3 - A_2C_3 \tag{22}$$

$$C_4 = A_2B_3 - B_2A_3 \tag{23}$$

Let $na_4 = \sqrt{A_4^2 + B_4^2 + C_4^2}$. The Z_{p2} axis is given by

$$A_5 = B_3C_4 - C_3B_4; B_5 = C_3A_4 - A_3C_4 \tag{24}$$

$$C_5 = A_3B_4 - B_3A_4 \tag{25}$$

Let $na_5 = \sqrt{A_5^2 + B_5^2 + C_5^2}$. The rotation matrix from $X_{p2}Y_{p2}Z_{p2}$ frame to the inertial frame is given by

$${}^{I}R_{P_2} = \begin{pmatrix} A_3 & \frac{A_4}{na_4} & \frac{A_5}{na_5} \\ B_3 & \frac{B_4}{na_4} & \frac{B_5}{na_5} \\ C_3 & \frac{C_4}{na_4} & \frac{C_5}{na_5} \end{pmatrix} \tag{26}$$

The kinematics of the MAV with respect to $X_{p2}Y_{p2}Z_{p2}$ frame is

$$\dot{x_{p2}} = V_a sin(\psi_2); \; \dot{y_{p2}} = V_a cos(\psi_2); \; z_{p2} = 0; \; \dot{\psi_2} = \frac{a_c}{V_a} \tag{27}$$

In the PL_2 plane, the path comprises of a small curve followed by a straight line and a circle (ref figure 4). The guidance logic for following the initial curved portion up to $1'$ and the straight line up to $(m_0, n_0, 0)$ is same as that followed in the PL_1 plane. The final portion will consist of a circle with radius greater than the minimum turn radius of the vehicle. In the figure 4, the centre of the circle is given by $(x_c, y_c, 0)$ and the line is tangent to the circle at the point $(m_0,n_0,0)$. So for the path segment (ref figure 4) from $(x_{01},y_{01},0)$ to $1'$ $a_c = k_1 d + k_2 \dot{d}$, for the path segment from $1'$ to $(m_0,n_0,0)$, $a_c = 0$ and for the final path segment from $(m_0,n_0,0)$ to $(x_2', y_2', 0)$, $a_c = \frac{V_a}{R}$. Equations 9 and 27 are to be solved numerically to obtain the co-ordinates in $X_{p1}Y_{p1}Z_{p1}$ and $X_{p2}Y_{p2}Z_{p2}$ frames. Then the rotation matrices ${}^I R_{P_1}$ and ${}^I R_{P_2}$ are used to obtain the inertial (X_I, Y_I, Z_I) coordinates of the path to be followed by the MAV to reach the goal point from the initial point.

A. Relation to PN guidance law

The PN guidance law [7] is given by

$$a_{Lospn} = N V_c \dot{\lambda} \tag{28}$$

where a_{Lospn} is the acceleration perpendicular to line of sight vector, V_c is the closing velocity, $\dot{\lambda}$ is the line of sight rate and N is the navigation constant. In figure 5, let M be the current position of the MAV, W be a point on the desired path, $X'Y'$ is parallel to $X_{p1}Y_{p1}$ if M is in PL_1 plane or parallel to X_{p2},Y_{p2} if M is in PL_2 plane, θ_m is the angle made by the velocity vector with the Y' axis, a_c is the applied acceleration and d is the miss distance. The acceleration component perpendicular to line of sight vector (r) is a_{Los}.

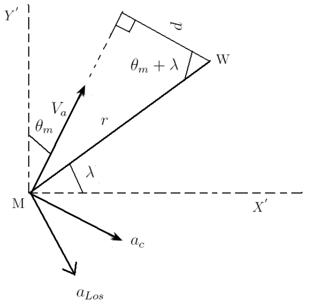

Fig. 5. Relation to PN guidance law

$$\dot{\lambda} = \frac{V_\lambda}{r} \; V_\lambda = -V_a cos(\theta_m + \lambda) \; V_c = -V_a sin(\theta_m + \lambda) \tag{29}$$

From the above equations,

$$a_{Lospn} = N \frac{V_a cos(\theta_m + \lambda) V_a sin(\theta_m + \lambda)}{r} \tag{30}$$

Since V_a is constant,

$$a_{Lospn} = N_1 \frac{cos(\theta_m + \lambda) sin(\theta_m + \lambda)}{r} \tag{31}$$

where $N_1 = N {V_a}^2$. For the guidance law in equation 12,

$$a_{Los} = a_c sin(\theta_m + \lambda) \tag{32}$$

$$a_{Los} = (k_1 d + k_2 \dot{d}) sin(\theta_m + \lambda) \tag{33}$$

$$d = r cos(\theta_m + \lambda) \tag{34}$$

$$\dot{d} = \dot{r} cos(\theta_m + \lambda) - r sin(\theta_m + \lambda)(\dot{\theta_m} + \dot{\lambda}) \tag{35}$$

After simplifying the above equations, we obtain

$$a_{Los} = \frac{k_3 r^2 a_{Lospn}}{1 - \frac{k_2 r \dot{r}}{{V_a}^2}} \tag{36}$$

where $k_3 = \frac{k_1}{N_1}$. As the goal point is approached, the guidance law is the scaled version of PN guidance law with the scaling factor as the quadratic function of range thus reducing the acceleration requirement. When switching from one goal point to another, the increase in the r^2 term in the numerator is compensated by the increase in $r\dot{r}$ term in the denominator, thus preventing the high acceleration demand. In general, if we choose $k_3 r^2 = 1 - \frac{k_2 r \dot{r}}{{V_a}^2}$, then the guidance law will be equal to PN guidance law.

III. IGC FRAMEWORK

In the conventional guidance and control system, the guidance logic forms the outer loop and control logic forms the inner loop. The control input takes a form of $U = F_c(X) + R_g$, where X are the MAV states (or output) and R_g is the reference from outer guidance loop like commanded heading, flight path angle or lateral acceleration. Thus the system input is computed in two steps. Where as in integrated guidance and control, the control input takes a form of $U = F_i(X) + G_i(d, \dot{d})$, where d is the miss distance and the control structure F_i and G_i are computed in one step. Here the entire path obtained through path planning algorithm is broken into discrete points along the path and each point is tracked one by one by the IGC algorithm. Since the discrete points are closer to each other, the kinematics are linearized. The commanded acceleration is approximated as $a_c \approx -\ddot{d}$, where d is the miss distance and can be obtained as follows. Let $a = (x,y,z)$ be the current MAV position, $n = (cos\psi cos\gamma, sin\psi cos\gamma, sin\gamma)$ be the current velocity vector and $p = (x_n, y_n, z_n)$ be the next point on the desired path. Let $d = (d_x, d_y, d_z)$ and is given by,

$$d \;\; = \;\; (a-p) - ((a-p).n)n \tag{37}$$

Let $e_1 = (x - x_n) cos\psi cos\gamma + (y - y_n) sin\psi cos\gamma + (z - z_n) sin\gamma$. Then the components of d can be written as

$$d_x = (x - x_n) - e_1 cos\psi cos\gamma \; d_y = (y - y_n) - e_1 sin\psi cos\gamma \tag{38}$$

$$d_z = (z - z_n) - e_1 sin\gamma \tag{39}$$

From the above equations $d = 0$ implies that $x = x_n$, $y = y_n$, $z = z_n$ or $x_n = x + k cos\psi cos\gamma$, $y_n = y + k sin\psi cos\gamma$, $z_n = z + k sin\gamma$, where k is a constant. This implies that the MAV has reached the desired point on the path or the velocity vector points towards the desired point. The objective of the IGC algorithm is to drive the miss distance, d to zero. Let the projection of d along the MAV pitch plane and yaw plane are d_1 and d_2 respectively. For the PL_1 plane, let the unit vector along the acceleration vector be (a_{m1}, b_{m1}, c_{m1}). In figure 6, XZ is the pitch plane of the MAV, X_B denotes the body X axis, α is the angle of attack, γ is the flight path angle and $V_a \dot{\gamma}$ is the acceleration perpendicular to the velocity vector in the pitch plane. The angle made by the acceleration vector with the X axis in the pitch plane is given by

$$\gamma_{a1} = tan^{-1}\left(\frac{(c_{m1})}{\sqrt{(a_{m1})^2 + (b_{m1})^2}}\right) \tag{40}$$

$$\ddot{d_1} = -a_c sin\gamma_{a1}, \; a_c sin\gamma_{a1} = V_a \dot{\gamma} cos\gamma \tag{41}$$

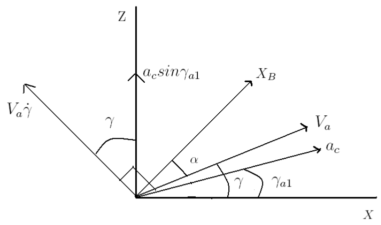

Fig. 6. Acceleration component in the pitch plane

Let $x_1 = d_1$, and $\dot{x_1} = x_2$. Then from the above equations,

$$\dot{x_2} = -V_a\dot{\gamma}cos\gamma \tag{42}$$

In figure 7, XY is the yaw plane of the MAV, X_B denotes the body X axis, β is the sideslip angle, ψ is the yaw angle and $V_a(\dot{\psi}+\dot{\beta})$ is the acceleration perpendicular to the velocity vector in the yaw plane. The angle made by the acceleration vector with the X axis in the yaw plane is given by

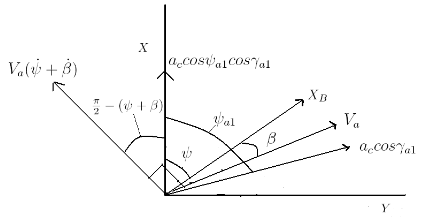
X
$a_c cos\psi_{a1} cos\gamma_{a1}$
$V_a(\dot{\psi}+\dot{\beta})$
$\frac{\pi}{2}-(\psi+\beta)$
X_B
ψ_{a1}
V_a
β
ψ
$a_c cos\gamma_{a1}$
Y

Fig. 7. Acceleration component in the yaw plane

$$\psi_{a1} = tan^{-1}(\frac{b_{m1}}{a_{m1}}),\ \ddot{d_2} = -a_c cos\gamma_{a1} \tag{43}$$

$$a_c\, cos\gamma_{a1} cos\psi_{a1} = V_a(\dot{\psi}+\dot{\beta})sin(\psi+\beta) - V_a\dot{\gamma}sin\gamma \tag{44}$$

$$a_c\, cos\gamma_{a1} sin\psi_{a1} = -V_a(\dot{\psi}+\dot{\beta})cos(\psi+\beta) \tag{45}$$

Let $x_3 = d_2$, and $\dot{x_3} = x_4$. Let $\psi+\beta = \chi$, and after simplifying the above equations,

$$\dot{x_4} = -V_a\sqrt{(\dot{\chi})^2 - 2(\dot{\chi})\,\dot{\gamma}sin\gamma sin(\chi) + (\dot{\gamma}sin\gamma)^2} \tag{46}$$

Since the applied acceleration is parallel to d,

$$d_1 = sin\gamma_{a1},\ d_2 = cos\gamma_{a1} \tag{47}$$

Similar equations holds for the path in the PL_2 plane.
The block diagram for integrated guidance and control is shown in figure 8. Here the path generation algorithm outputs the discrete coordinates (x_n, y_n, z_n) to be followed by the MAV. The input to the IGC algorithm are the MAV outputs $[a_x, a_y, a_z, p, q, r, \psi, V_a, x, y, z]^T$ and the discrete coordinates (x_n, y_n, z_n). Here (a_x, a_y, a_z) are the acceleration along the MAV body axis, (p, q, r) are the roll rate, pitch rate and yaw rate respectively, ψ the yaw angle, V_a is the airspeed and (x, y, z) is the current position of the MAV. The IGC algorithm computes $[x_1, x_2, x_3, x_4]$ as explained in the equations from 37 to 47. The output of the IGC algorithm are $U = [U_{\delta e}, U_{\delta r}, U_{Th}]^T$, where $U_{\delta e}$ is the elevator input, $U_{\delta r}$ is the rudder input and U_{Th} is the throttle input. Let (u, v, w) be the body frame velocity components of the MAV and (ϕ, θ, ψ) be the Euler angles. Let the operating point of the MAV be given by $(u^*, v^*, w^*, p^*, q^*, r^*, \phi^*, \theta^*, \psi^*)$. Then the linear state space model with state variables $X = [u, v, w, p, q, r, \phi, \theta, x_1, x_2, x_3, x_4]^T$ can be written as

$$\dot{X} = AX + BU,\ Y = CX \tag{48}$$

where $Y = [a_x, a_y, a_z, p, q, r, V_a, x_1, x_2, x_3, x_4]^T$ and $U = [U_{\delta e}, U_{\delta r}, U_{Th}]^T$. The A,B,C matrices are of dimensions 12x12, 12x3 and 11x12 respectively [8]. The controller has the following structure

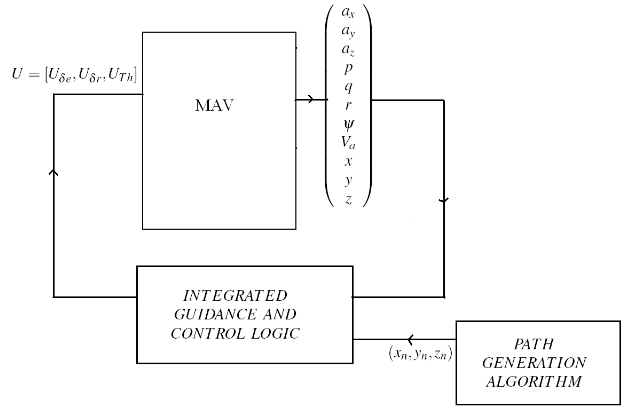
$U = [U_{\delta e}, U_{\delta r}, U_{Th}]$
MAV
a_x
a_y
a_z
p
q
r
ψ
V_a
x
y
z
INTEGRATED GUIDANCE AND CONTROL LOGIC
(x_n, y_n, z_n)
PATH GENERATION ALGORITHM

Fig. 8. Block diagram for IGC framework for path following

$$U_{\delta e} = k_{11}a_x + k_{12}a_z + k_{13}q + k_{14}V_a + k_{15}x_1 + k_{16}x_2 \tag{49}$$

$$U_{\delta r} = k_{21}a_y + k_{22}p + k_{23}r + k_{24}V_a + k_{25}x_3 + k_{26}x_4 \tag{50}$$

$$U_{Th} = k_{31}a_x + k_{32}a_z + k_{33}q + k_{34}V_a + k_{35}x_1 + k_{36}x_2 \tag{51}$$

where k_{ij} are the feedback gains. Here the longitudinal variables are fed back to the elevator and throttle and the lateral variables are fed back to the rudder. When there is a strong coupling between the longitudinal and lateral dynamics, both the longitudinal and lateral variables are to be fed back to all the three control inputs. The objective is to drive x_1 and x_3 to zero and maintain the desired airspeed, V_a .

IV. SIMULATION RESULTS

The MAV considered here [8] is of 150 mm span, with a minimum turn radius of 20m and maximum climb rate of 1.5m/s at a velocity of 12m/s. The initial position of the MAV is $(x_0 = 100m, y_0 = 10m, z_0 = 100m)$ and heading $\psi_0 = 0°$ and flight path angle $\gamma_0 = 5°$. The next waypoint position is $(x_f = 500m, y_f = 140m, z_f = 130m)$ and heading $\psi_f = 60°$ and flight path angle $\gamma_f = 0°$. The path generated using the algorithm is shown in figure 9. The red colored portion shows the generated path in the PL_1 plane and the blue colored portion shows the path in the PL_2 plane. The heading and flight path angle are shown in figures 10 and 11 respectively. We can see that in the PL_1 plane, the path is curved one and in the PL_2 plane the path is mostly a straight line followed by a curve at the end. The non linear six degree of freedom simulation of the MAV flight for path following using integrated guidance and control logic is shown in figure 12. The initial position of the MAV is $(x_0 = 100m, y_0 = 10m, z_0 = 0m)$ and the final waypoint position is $(x_0 = 145m, y_0 = 40m, z_0 = 0m)$. The red curve shows the generated path and the blue curve shows the path followed by the MAV. The dots on the red curve are the discrete waypoint inputs to the integrated guidance and control logic. The airspeed is shown in figure 13 and is almost constant.

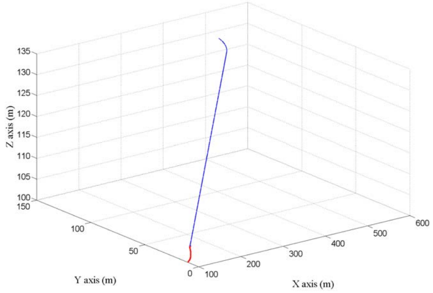

Fig. 9. Generated path in 3D space

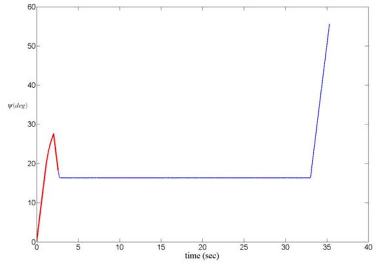

Fig. 10. Heading angle for the generated path in 3D space

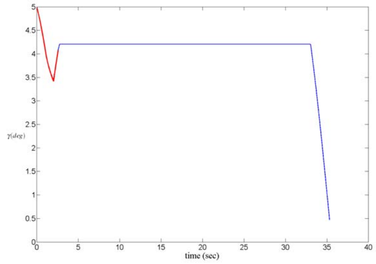

Fig. 11. Flight path angle for the generated path in 3D space

V. CONCLUSIONS

A new method for generating path connecting the waypoints in the three dimensional space has been discussed. The method is computationally efficient and can be used to generate path online during flight. The simulation results shows that, the generated path comprises of curves and straight lines in which straight line occupies the major portion, thus reducing the overall path length. The guidance law used here is a modified version of PN guidance law. The IGC framework developed here combines the guidance and control logic into a single loop design. This relaxes the requirement for time scale separation between the states used in the conventional successive loop closure design.

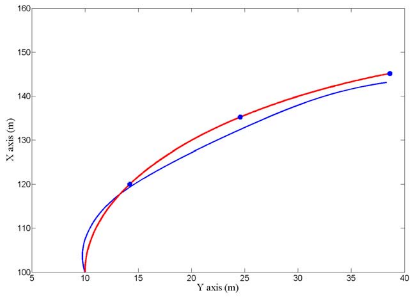

Fig. 12. Path following in 2D

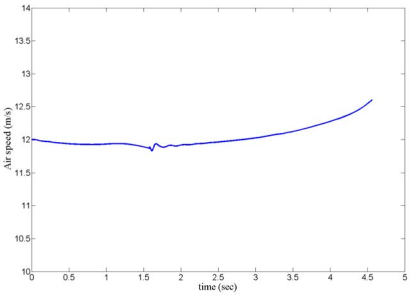

Fig. 13. Air speed variation for path following in 2D

ACKNOWLEDGMENT

The authors would like to thank DRDO and ARDB for their support for the project and Mr.Arun Joseph for his support in performing the simulations.

REFERENCES

[1] A. R. Babaei and M. Mortazavi, Three-Dimensional Curvature-Constrained Trajectory Planning Based on In-Flight Waypoints, Journal of Aircraft, vol. 47, No.4, July-August 2010, pp. 1391-1398.

[2] E. D. B. Medagoda and P. W. Gibbens, Synthetic-Waypoint Guidance Algorithm for Following a Desired Flight Trajectory, Journal of Guidance Control and Dynamics, Vol.33, No.2, March-April 2010, pp. 601-606.

[3] K.Bousson and P.Machado, 4D Flight Trajectory Optimization Based on Pseudospectral Methods, World Academy of Science Engineering and Technology, Vol.45, 2010, pp. 551-557.

[4] G. Ambrosino, M. Ariola, U. Ciniglio, F. Corraro, E. De Lellis and A. Pironti, Path Generation and Tracking in 3-D for UAVs, IEEE transactions on Control Systems Technology, Vol.17, No.4, July 2009, pp. 980-988.

[5] S.Hota and D.Ghose, Optimal Path Planning for an Aerial Vehicle in 3D Space, IEEE Conference on Decision and Control,December 2010, pp. 4902-4907.

[6] I.Kaminer, A.Pascal, E.Hallberg and C.Silvestre, Trajectory Tracking for Autonomous Vehicles: An Integrated approach to Guidance and Control, Journal of Guidance Control and Dynamics, Vo.21, 1998, pp. 29-38.

[7] P. Zarchan, Tactical and Strategic Missile guidance, second edition, AIAA, 1994, pp. 25-43.

[8] M.S.Bhat, S.N.Omkar, K.Harikumar, T.Bera, E.A.George, S.Dhall and A.Joseph, Development of Autonomous Robust Fixed Wing Micro Air Vehicle, DRDO technical report No: AE/MSB/DRDO-NPMICAV-TR-2012-001, December 2012.